Science REPORTS

Cite as: K.-H. Kim et al., Science 10.1126/science.aat6081 (2018).

Assessing whether the 2017 M_w 5.4 Pohang earthquake in South Korea was an induced event

Kwang-Hee Kim,[1]* Jin-Han Ree,[2]* YoungHee Kim,[3] Sungshil Kim,[2] Su Young Kang,[1] Wooseok Seo[1]

[1]Department of Geological Science, Pusan National University, Busan 46241, Republic of Korea. [2]Department of Earth and Environmental Sciences, Korea University, Seoul 02841, Republic of Korea. [3]School of Earth and Environmental Sciences, Seoul National University, Seoul 08826, Republic of Korea.

*Corresponding author. Email: kwanghee@pusan.ac.kr (K.-H.K.); reejh@korea.ac.kr (J.-H.R.)

The M_w 5.4 Pohang earthquake, the most damaging event in South Korea since instrumental seismic observation began in 1905, occurred beneath the Pohang geothermal power plant in 2017. Geological and geophysical data suggest that the Pohang earthquake was induced by fluid from an enhanced geothermal system (EGS) site, which was injected directly into a near-critically-stressed subsurface fault zone. The magnitude of the mainshock makes it the largest known induced earthquake at an EGS site.

The injection of fluid into reservoir rocks, which facilitates oil and gas recovery, enhances geothermal systems, and aids in the disposal of waste water and CO_2 gas, also has a small chance of inducing earthquakes (e.g., *1*–*4*). Empirical and theoretical relationships exist to connect the maximum magnitude of an induced earthquake and the injected fluid volume (*2*, *5*). The magnitude of an induced earthquake may be tectonically controlled. This may be due to the presence of a fault suitably oriented for slip under a given stress field that is also located adjacent to one or more injection or production wells (*6*, *7*). The earthquake nucleation itself might be controlled by the injection (*6*). Previously observed magnitudes of induced seismicity at enhanced geothermal systems (EGS) sites are relatively small (*8*); the largest local magnitude (M_L) reported was a M_L 3.4 at Basel, Switzerland (*9*), although a much larger, possibly induced earthquake has been reported in geothermal fields of tectonically active area (*10*).

An M_w 5.4 earthquake occurred at the Pohang EGS site in southeastern Korea on 15 November 2017. The earthquake was the most damaging in South Korea since the first seismograph was installed in 1905, and the second-largest in magnitude since 1978 when scientific instrumental observations began. The earthquake injured ninety people and the estimated property damage was US$52 million (*11*). We present evidence that suggests the Pohang earthquake is the largest induced event at any EGS site worldwide. Moreover, this event indicates that injected fluid volumes much smaller than predicted by theory can trigger a relatively large earthquake, at least under the right set of conditions.

The Korean Peninsula lies within the Eurasian Plate (Fig. 1), although it was comprised of continental magmatic arcs at a plate boundary until the early Tertiary (~30 million years ago) (*12*). NNE-striking strike-slip faults and NNE- to NE-striking normal faults developed predominantly in southeast Korea and adjacent offshore areas when the East Sea (or Japan Sea) opened as a back-arc basin in the early to middle Tertiary (30~15 million years ago), with the coetaneous formation of smaller-scale basins, including the Pohang Basin (*12*–*14*). Some of these faults have been reactivated as strike-slip and thrust faults in the current compressional regime (*13*–*15*). The axes of compression determined by focal mechanism solutions indicate shallow plunges to the ENE throughout the southern Korean Peninsula (*15*, *16*).

The Pohang Basin consists of Miocene (~20 million years ago) non-marine to deep marine sedimentary strata with basement rocks of Cretaceous to Eocene sedimentary and volcanic rocks and late Paleozoic to Eocene granitoids (*17*–*19*) (Fig. 2A). The geology of the Pohang EGS site comprises (from top to bottom) Quaternary alluvia (<10 m thick), Miocene semi-consolidated mudstone (200–400 m thick), Cretaceous to Eocene sedimentary and igneous rocks (~1,000 m thick), and Permian granodiorite with gabbroic dykes (*19*–*21*) (Fig. 2B). One vertical injection well (4,382 m deep; PX2) and another deviated production well (4,348 m deep; PX1) were drilled into Permian granodiorite with gabbroic dykes for the EGS, with an expected electricity production of 1.2 megawatts (*21*). The PX1 well, only 6 m from PX2 at the surface, is 600 m northwest of PX2 at the bottom (Fig. 3). The drilling began in September 2012 and was completed in November 2015. No M_L >2.0 earthquakes were recorded within 10 km of the Pohang EGS site between 1978 and 2015 (*22*); only six earthquakes with M_L 1.2–1.9 were detected in the area between 2006 and 2015. To further examine the seismicity around the EGS site, we improved the earthquake catalog by applying a single-station matched filter to continuous waveforms (*23*) recorded by a permanent seismic station (PHA2, Fig. 2A) located about 10 km north of the site, for the period between 1 January 2012 and 14 November 2017. Once detected, waveforms were visually inspected for time differences between P and S wave arrivals consistent with a source at Pohang (~1.54 s). The matched filter analysis found no noticeable earthquakes at the EGS site before the completion of drilling. We detected a total of 150 earthquakes by the match filtering that all occurred after the completion of the drilling, including 4 additional earthquakes with M_L > 2.0.

Hydraulic stimulation began on 29 January 2016 and comprised four phases of injection with a total volume of 12,800 m^3 at injection rates of 1.00 to 46.83 l s^{-1} (Fig. 4). Fluid was injected into both PX1 (phases 2 and 3) and PX2 (phases 1, 3, and 4). To investigate the relationship between seismicity and fluid injection, we used regional earthquakes detected by the matched filter together with those provided by the Pohang EGS project team (*23*). We did not detect noticeable microearthquake before the drilling. The timing of the earthquakes coincides with the well completing, despite a lack of reported fluid injection or bleed-off. The first reported hydraulic stimulation (Phase 1) was carried out between 29 January 2016 and 20 February 2016, followed by three additional phases of fluid injection (Fig. 4). Each injection phase was accompanied by intense seismic activity that started only a few days after injection. Microseismic activity decreased rapidly after the termination of fluid injection. The magnitudes of induced earthquakes tend to increase with an increase in the net volume of injected fluid. After an M_L 3.1 earthquake on 15 April 2017, which was the largest felt event near the EGS site before the M_L 5.4 Pohang earthquake, we deployed eight temporary seismic stations around the EGS site. Each standalone station was equipped with a 3-component velocity type short-period sensor. They record continuous seismic data at a sampling frequency of 200 Hz. Installation was completed on 10 November 2017. All of them are still in active operation.

The M_L 5.4 mainshock occurred at the Pohang EGS site on 15 November 2017, and was preceded and followed by foreshocks and aftershocks, respectively, all of which were well-recorded by our local seismic array at distances of 0.6–2.5 km from the mainshock epicenter (Figs. 2A and 3). We precisely relocated this earthquake sequence with the *hypoDD* software package (*23*, *24*) (fig. S2). We plotted the spatial distribution of six foreshocks (M_L ≤ 2.6), the mainshock, and 210 aftershocks that occurred within three hours of the mainshock (Fig. 3). The first two foreshocks occurred about 9 hours before the mainshock; the remaining four preceded it by 6–7 min. Most hypocentral depths fall in the range 4–6 km and the mainshock depth is about 4.5 km. Of note, the hypocenters of the foreshocks and mainshock are located immediately adjacent to the bottom of PX1. The hypocentral depths of the Pohang earthquake sequence are shallower than most earthquakes in the Korean Peninsula, which tend to occur at depths of 10–20 km (*25*). For comparison, the largest instrumentally recorded earthquake in South Korea, the 2016 Gyeongju event (M_L 5.8), had a hypocentral depth of about 14 km (*26*). The spatio-temporal distribution of hypocenters indicates that the rupture plane consisted of two segments, a principal southwestern segment and a subsidiary northeastern segment in geographic location (Fig. 3 and fig. S3). The aftershocks tend to occur earlier on the main segment than on the subsidiary segment (fig. S4). This observation, together with the locations of the foreshocks and mainshock on the main segment, suggests that the main segment ruptured earlier than the subsidiary one. We determined the best-fit orientations of the main and subsidiary rupture planes by statistical plane-fitting using *Mathworks MATLAB* software, are N36°E (strike)/65°NW (dip) and N19°E/60°NW, respectively (fig. S3). These orientations are consistent with the nodal planes determined by focal mechanism solutions (Fig. 3). The main segment shows thrust faulting with a minor strike-slip component, whereas the subsidiary segment is dominated by strike-slip faulting with a minor dip-slip component. The compression axis trends E–W or ENE–WSW with a shallow plunge, similar to that of other earthquakes in South Korea (*15*, *16*). The locations of the foreshocks and mainshock, at the bottom of the injection well, suggest that fluid was injected directly into the fault zone.

The temporal relationship between seismicity and fluid injection, the spatial relationship between the hypocenters and the EGS site, and the lack of seismicity in the area before the EGS all suggest that the Pohang earthquake was induced. Furthermore, the immediate response of seismicity to fluid injection and the locations of foreshocks and mainshock at the bottom of the injection well suggest that fluid was injected directly into a fault zone. The fault plane inferred from the spatial distribution of hypocenters and focal mechanism solutions strikes NE and dips to the NW (fig. S4A), similar to Quaternary thrust faults in southeastern Korea. In fact, a magnetotelluric (MT) survey of the EGS site detected a low-resistivity feature that could be the fault zone, striking NE and dipping to the NW (*23*, *27*; fig. S5). Reverse slip along a subsurface fault is consistent with the current stress field. All these lines of evidence indicate that the Pohang earthquake is “probably induced” to “almost certainly induced” in Frohlich’s system of assessment (*28*). If we use McGarr’s (*2*) equation for the relationship between the maximum magnitude and the total volume of injected fluid, about 4.7 × 10^6 m^3 of injected fluid would be required to induce an M_w 5.4 earthquake, which is more than 810 times the fluid injected at the Pohang EGS site. The permeability structure of fault zones is highly heterogeneous, and patches or layers of clay-rich gouge within the fault core act as barriers to fluid flow (*29*). The pore pressure thus can reach a critical value locally for earthquake nucleation after injecting a relatively small volume of fluid, depending on fault zone structure. Our results imply that if fluid is injected directly into a near-critically-stressed fault, it can induce a larger earthquake than current theory predicts. Detailed investigation of the geological, geochemical, and geophysical properties of the Pohang EGS site will provide a unique opportunity to improve our understanding of earthquake-inducing processes.

REFERENCES AND NOTES

1. W. L. Ellsworth, Injection-induced earthquakes. *Science* **341**, 1225942 (2013). doi:10.1126/science.1225942 Medline
2. A. McGarr, Maximum magnitude earthquakes induced by fluid injection. *J. Geophys. Res. Solid Earth* **119**, 1008–1019 (2014). doi:10.1002/2013JB010597
3. A. Zang, V. Oye, P. Jousset, N. Deichmann, R. Gritto, A. McGarr, E. Majer, D. Bruhn, Analysis of induced seismicity in geothermal reservoirs – An overview. *Geothermics* **52**, 6–21 (2014). doi:10.1016/j.geothermics.2014.06.005
4. M. D. Zoback, S. M. Gorelick, Earthquake triggering and large-scale geologic storage of carbon dioxide. *Proc. Natl. Acad. Sci. U.S.A.* **109**, 10164–10168 (2012). doi:10.1073/pnas.1202473109 Medline
5. A. McGarr, Seismic moments and volume changes. *J. Geophys. Res. Solid Earth* **81**, 1487–1494 (1976). doi:10.1029/JB081i008p01487
6. N. J. van der Elst, M. T. Page, D. A. Weiser, T. H. W. Goebel, S. M. Hosseini, Induced earthquake magnitudes are as large as (statistically) expected. *J. Geophys. Res. Solid Earth* **121**, 4575–4590 (2016). doi:10.1002/2016JB012818
7. E. L. Majer, R. Baria, M. Stark, S. Oates, J. Bommer, B. Smith, H. Asanuma, Induced seismicity associated with Enhanced Geothermal Systems. *Geothermics* **36**, 185–222 (2007). doi:10.1016/j.geothermics.2007.03.003
8. G. Grünthal, Induced seismicity related to geothermal projects versus natural tectonic earthquakes and other types of induced seismic events in Central Europe. *Geothermics* **52**, 22–35 (2014). doi:10.1016/j.geothermics.2013.09.009
9. M. O. Häring, U. Schanz, F. Ladner, B. C. Dyer, Characterisation of the Basel 1 enhanced geothermal system. *Geothermics* **37**, 469–495 (2008). doi:10.1016/j.geothermics.2008.06.002
10. D. T. Trugman, A. A. Borsa, D. T. Sandwell, Did stress from the Cerro Prieto Geothermal Field influence the El Mayor-Cucapah rupture sequence? *Geophys. Res. Lett.* **41**, 8767–8774 (2014). doi:10.1002/2014GL061959
11. National Disaster and Safety Status Control Center, Ministry of the Interior and Safety, Republic of Korea, press release (6 December 2017).
12. S. K. Chough, S.-T. Kwon, J.-H. Ree, D. K. Choi, Tectonic and sedimentary evolution of the Korean peninsula: A review and new view. *Earth Sci. Rev.* **52**, 175–235 (2000). doi:10.1016/S0012-8252(00)00029-5
13. J.-H. Ree, Y.-J. Lee, E. J. Rhodes, Y. Park, S.-T. Kwon, U. Chwae, J.-S. Jeon, B. J. Lee, Quaternary reactivation of Tertiary faults in southeastern Korean Peninsula: Age constraint by optically stimulated luminescence dating. *Isl. Arc* **12**, 1–12 (2003). doi:10.1046/j.1440-1738.2003.00372.x
14. S. H. Yoon, Y. K. Sohn, S. K. Chough, Tectonic, sedimentary, and volcanic evolution of a back-arc basin in the East Sea (Sea of Japan). *Mar. Geol.* **352**, 70–88 (2014). doi:10.1016/j.margeo.2014.03.004
15. H. Choi, T.-K. Hong, X. He, C.-E. Baag, Seismic evidence for reverse activation of a paleo-rifting system in the East Sea (Sea of Japan). *Tectonophysics* **572–573**, 123–133 (2012). doi:10.1016/j.tecto.2011.12.023
16. J.-C. Park, W. Kim, T. W. Chung, C.-E. Baag, J.-H. Ree, Focal mechanisms of recent earthquakes in the southern Korean Peninsula. *Geophys. J. Int.* **169**, 1103–1114 (2007). doi:10.1111/j.1365-246X.2007.03321.x
17. Y. K. Sohn, C. W. Rhee, H. Shon, Revised stratigraphy and reinterpretation of the Miocene Pohang basinfill, SE Korea: Sequence development in response to tectonism and eustasy in a back-arc basin margin. *Sediment. Geol.* **143**, 265–285 (2001). doi:10.1016/S0037-0738(01)00100-2
18. Y. K. Sohn, M. Son, Synrift stratigraphic geometry in a transfer zone coarse-grained delta complex, Miocene Pohang Basin, SE Korea. *Sedimentology* **51**, 1387–1408 (2004). doi:10.1111/j.1365-3091.2004.00679.x
19. T. J. Lee, Y. Song, D.-W. Park, J. Jeon, W. S. Yoon, "Three dimensional geological model of Pohang EGS pilot site, Korea", in *Proceedings of the World Geothermal Congress*, Melbourne, Australia, 19 to 25 April 2015; https://pangea.stanford.edu/ERE/db/WGC/papers/WGC/2015/31025.pdf.
20. K.-S. Yoon, J.-S. Jeon, H.-K. Hong, H.-G. Kim, A. Hakan, J.-H. Park, W.-S. Yoon, "Deep drilling experience for Pohang Enhanced Geothermal Project in Korea," in *Proceedings of the World Geothermal Congress*, Melbourne, Australia, 19 to 25 April 2015; https://pangea.stanford.edu/ERE/db/WGC/papers/WGC/2015/06034.pdf.
21. M. Kim, B. Yoon, C. Lee, K. G. Park, W.-S. Yoon, Y. Song, T. J. Lee, "Microseismic monitoring during hydraulic stimulation in Pohang (Korea) for EGS pilot project" [abstract S23B-0804], American Geophysical Union Fall Meeting, New Orleans, LA, USA, 11 to 15 December 2017.
22. The KMA (Korea Meteorological Administration) catalog is available at http://necis.kma.go.kr/.
23. Supplementary materials.
24. F. Waldhauser, W. L. Ellsworth, Double-difference earthquake location algorithm: Method and application to the Northern Hayward Fault, California. *Bull. Seismol. Soc. Am.* **90**, 1353–1368 (2000). doi:10.1785/0120000006
25. Korea Meteorological Administration earthquake data service, www.weather.go.kr/weather/earthquake_volcano/domesticlist.jsp
26. K.-H. Kim, T.-S. Kang, J. Rhie, Y. Kim, Y. Park, S. Y. Kang, M. Han, J. Kim, J. Park, M. Kim, C. Kong, D. Heo, H. Lee, E. Park, H. Park, S.-J. Lee, S. Cho, J.-U. Woo, S.-H. Lee, J. Kim, The 12 September 016 Gyeongju earthquakes: 2. Temporary seismic network for monitoring aftershocks. *Geosci. J.* **20**, 753–757 (2016). doi:10.1007/s12303-016-0034-9
27. T. J. Lee, Y. Song, T. Uchida, Two-dimensional interpretation of far-remote reference magnetotelluric data for geothermal application. *Butsuri Tansa* **8**, 145–155 (2005) (in Korean with English abstract).
28. C. Frohlich, H. DeShon, B. Stump, C. Hayward, M. Hornbach, J. I. Walter, A historical review of induced earthquakes in Texas. *Seismol. Res. Lett.* **87**, 1022–1038 (2016). doi:10.1785/0220160016
29. J. S. Caine, J. P. Evans, C. B. Forster, Fault zone architecture and permeability structure. *Geology* **24**, 1025–1028 (1996). doi:10.1130/0091-7613(1996)024<1025:FZAAPS>2.3.CO;2
30. T. Seno, S. Stein, A. E. Gripp, A model for the motion of the Philippine Sea Plate consistent with NUVEL-1 and geological data. *J. Geophys. Res. Solid Earth* **98**, 17941–17948 (1993). doi:10.1029/93JB00782
31. S. J. Gibbons, F. Ringdal, The detection of low magnitude seismic events using array-based waveform correlation. *Geophys. J. Int.* **165**, 149–166 (2006). doi:10.1111/j.1365-246X.2006.02865.x
32. M. Han, K.-H. Kim, M. Son, S. Y. Kang, Current microseismicity and generating faults in the Gyeongju area, southeastern Korea. *Tectonophysics* **694**, 414–423 (2017). doi:10.1016/j.tecto.2016.11.026
33. D. P. Schaff, F. Waldhauser, One magnitude unit reduction in detection threshold by cross correlation applied to Parkfield (California) and China seismicity. *Bull. Seismol. Soc. Am.* **100**, 3224–3238 (2010). doi:10.1785/0120100042
34. J. C. Lahr, HYPOELLIPSE: A computer program for determining local earthquake hypocentral parameters, magnitude, and first-motion pattern (Y2K Compliant Version) (Open-File Report 99–23, U.S. Geological Survey, 1999).
35. W. Kim, P-wave velocity structure of upper crust in the vicinity of the Yangsan Fault region. *Geosci. J.* **3**, 17–22 (1999). doi:10.1007/BF02910230
36. S. Hwang, I. H. Park, S. Yoonho, Interpretation of geophysical well logs from deep geothermal borehole in Pohang. *Mulli-Tamsa* **10**, 332–344 (2007).
37. J. Gomberg, K. M. Shedlock, S. W. Roecker, The effect of S-wave arrival on the accuracy of hypocenter estimation. *Bull. Seismol. Soc. Am.* **80**, 1605–1628 (1990).

ACKNOWLEDGMENTS

We thank Representative Sung Soo Kim of the National Assembly and the Ministry of Trade, Industry and Energy, Republic of Korea for providing fluid injection data to us. We also thank two anonymous reviewers for their constructive comments. **Funding:** This work was supported by the Nuclear Safety Research Program through the Korea Foundation of Nuclear Safety (KoFONS) using financial resources granted by the Nuclear Safety and Security Commission (NSSC) of the Republic of Korea (No. 1705010) and the Korea Meteorological Administration Research Development Program (No. KMI2018-02801). **Author contributions:** K.-H.K.: Conceptualization, Formal analysis, Funding acquisition, Methodology, Original draft, Review & editing; J.-H.R.: Conceptualization, Formal

analysis, Funding acquisition, Methodology, Original draft, Review & editing; Y.K.: Investigation, Methodology, Validation, Review & editing; S.K: Data curation, Formal analysis, Investigation, Software; S.Y.K.: Data curation, Formal analysis, Investigation, Software; W.S.: Data curation, Formal analysis, Investigation, Software; **Competing interests:** All authors declare no conflicts of interest. **Data and materials availability:** Our earthquake catalog including earthquake source parameters (location and time) and waveforms used in the paper are available at https://zenodo.org/record/1218738#.WtPQROTEaRE. Earthquake waveform data recorded at PHA2 can be acquired from the National Earthquake Comprehensive Information System, Korea Meteorological Administration (http://necis.kma.go.kr/, last accessed in April 2018). Continuous data may be obtained from the website upon request.

SUPPLEMENTARY MATERIALS

www.sciencemag.org/cgi/content/full/science.aat6081/DC1
Materials and Methods
Figs. S1 to S5
References (*31*–*37*)

18 March 2018; accepted 16 April 2018
Published online 26 April 2018
10.1126/science.aat6081

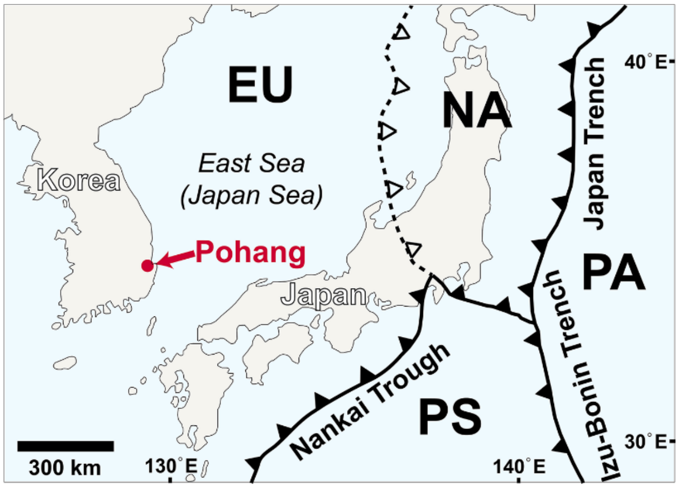

Fig. 1. Tectonic map of northeast Asia. Saw-toothed lines with solid teeth denote subduction zones. The broken line with open teeth represents an incipient subduction zone (*30*). EU: Eurasian Plate. NA: North American Plate. PS: Philippine Sea Plate. PA: Pacific Plate.

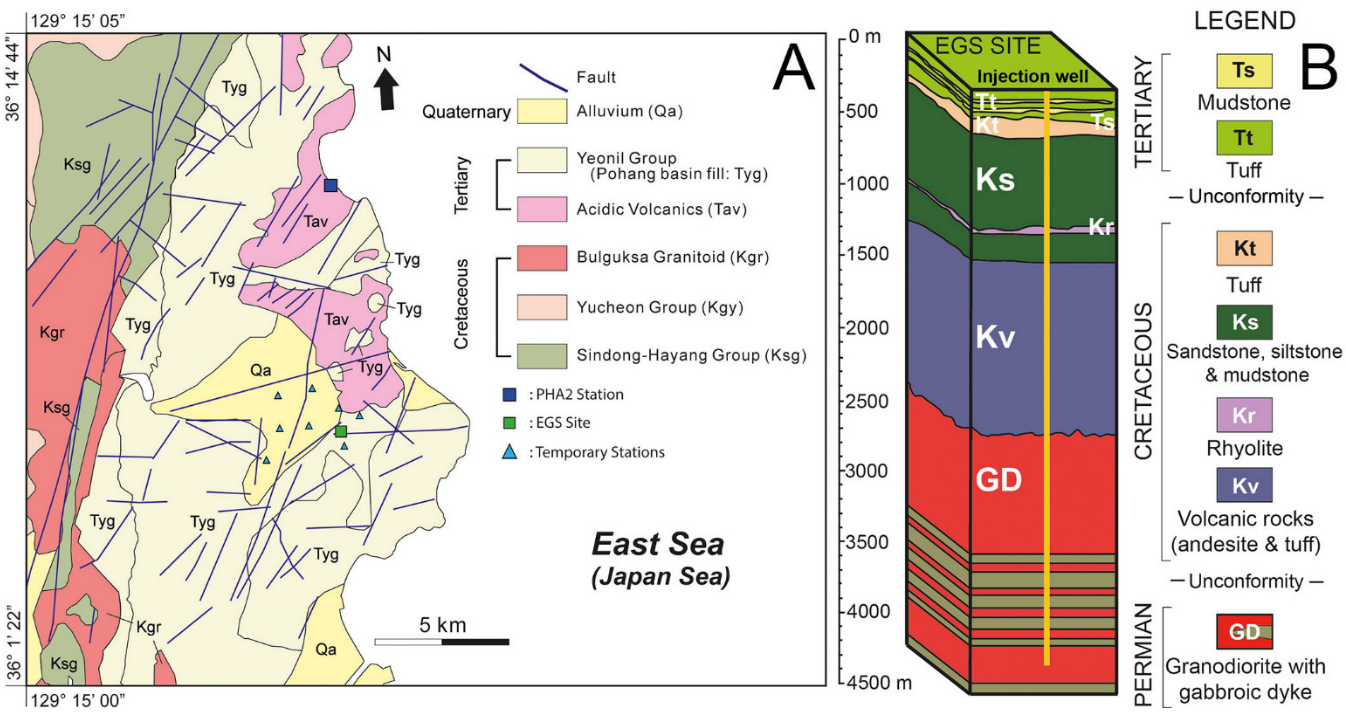

Fig. 2. Geologic map and column of the Pohang Basin. (**A**) Map showing rock sequences and faults of the Pohang Basin and adjacent area. One permanent seismic station operated by the Korea Meteorological Administration (PHA2) and our eight temporary seismic stations are represented by a dark blue square and green triangles, respectively. The green square denotes the site of the Pohang enhanced geothermal system (EGS). The geologic map was compiled from (18, 19). (**B**) Geologic column of the Pohang EGS site with injection well. The geologic column is compiled from (*19*, *20*).

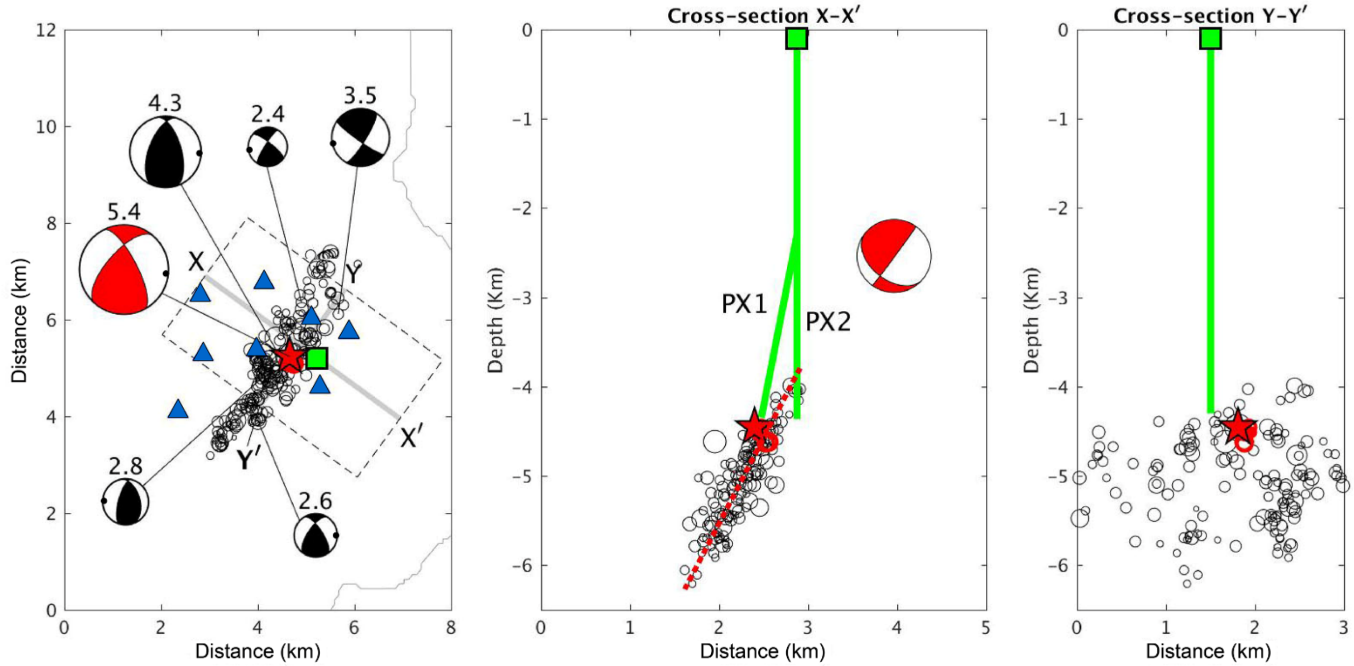

Fig. 3. Spatial distribution of epicenters and hypocenters of the 2017 Pohang earthquake sequence. (**A**) Epicenters of six foreshocks (red circles), mainshock (red star), and 210 aftershocks (small open circles) recorded in the first three hours after the mainshock. The location of the Pohang enhanced geothermal system (EGS) is indicated by a green square. Red beach ball with magnitude represents the source mechanism of the mainshock. Other black beach balls show the focal mechanism solutions of representative aftershocks. The black beach balls of the M_L 2.4 and 3.5 aftershocks, recorded one and three days after the mainshock, respectively, show strike-slip faulting more clearly. X–X' and Y–Y' denote the locations of the cross-sections shown in (B) and (C), respectively. (**B** and **C**) Hypocentral distributions of earthquakes projected onto vertical planes along lines X–X' (B) and Y–Y' (C) shown in (A). Red beach ball in (B) represents the focal mechanism of the mainshock projected onto a vertical cross-section. PX1 and PX2 denote production and injection wells, respectively. Other symbols are the same as for (A).

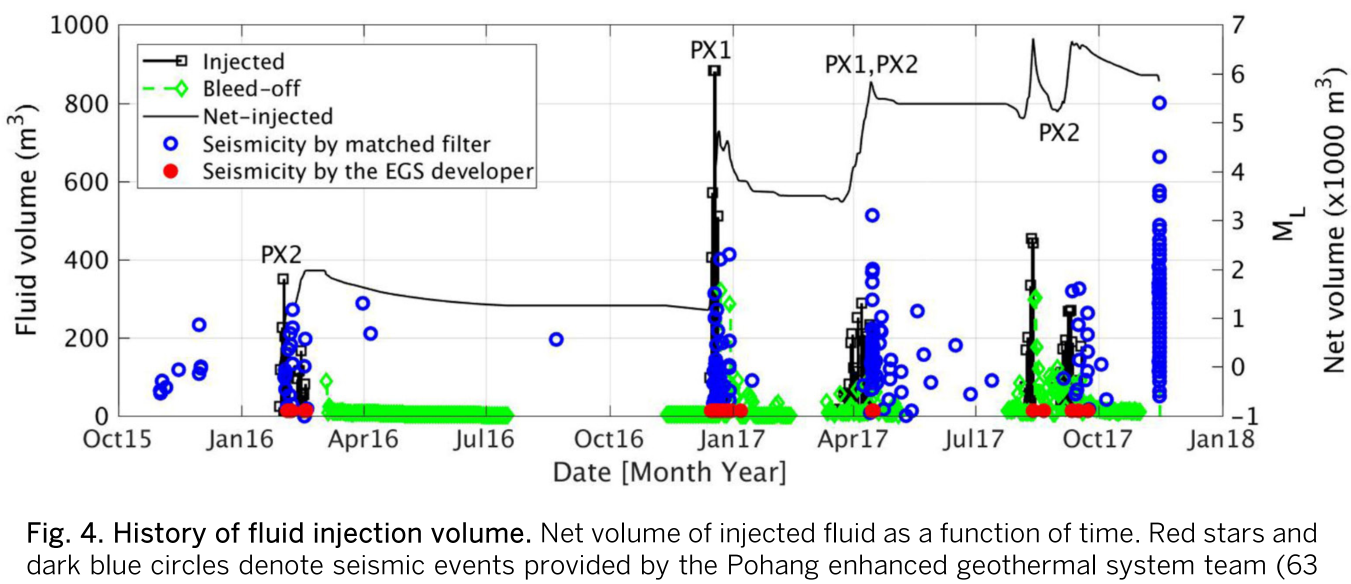

Fig. 4. History of fluid injection volume. Net volume of injected fluid as a function of time. Red stars and dark blue circles denote seismic events provided by the Pohang enhanced geothermal system team (63 events) and determined by matched filter analysis (150 events), respectively. Numbered red scale at right gives local magnitudes (M_L) of seismic events.

Science

Assessing whether the 2017 M_W 5.4 Pohang earthquake in South Korea was an induced event

Kwang-Hee Kim, Jin-Han Ree, YoungHee Kim, Sungshil Kim, Su Young Kang and Wooseok Seo

published online April 26, 2018